# Fluorescent probes based on side-chain chlorinated benzo[*a*]phenoxazinium chlorides: studies of interaction with DNA

B. Rama Raju,[a,b] M. Sameiro T. Gonçalves[a] and Paulo J. G. Coutinho[*b]

[a]*Centre of Chemistry, University of Minho, Campus de Gualtar, 4710-057 Braga, Portugal.* [b]*Centre of Physics, University of Minho, Campus de Gualtar, 4710-057 Braga, Portugal.*
**Corresponding author. Phone: +351 253604321; fax +351 253604061.*
*E-mail address: pcoutinho@fisica.uminho.pt*

## Abstract

The interaction of DNA with six water soluble benzo[*a*]phenoxazinium chlorides mono- or di-substituted with 3-chloropropyl groups at the *O* and *N* of 2- and 9-positions, along with methyl, hydroxyl and amine terminal groups at 5-positions, was investigated by photophysical techniques. The results indicated that almost all compounds intercalated in DNA base pairs at phosphate to dye ratio higher than 5. At lower values of this ratio, electrostatic binding mode with DNA was observed. Groove binding was detected mainly for the benzo[*a*]phenoxazinium dye with $NH_2$.HBr terminal. The set of six benzo[*a*]phenoxazinium chlorides proved successful to label the migrating DNA in agarose gel electrophoresis assays. These finding proves the ability of these benzo[*a*]phenoxazinium dyes to strongly interact with DNA.

*Keywords*: Nile Blue; Benzo[*a*]phenoxazinium chlorides; Fluorescent probes; DNA interaction; Fluorescence anisotropy; Gel electrophoresis

## 1. Introduction

Small fluorescent molecules serve as important tools in quantification and identification of living cells and organisms [1]. They also find numerous applications in drug delivery [2], sensing [3], monitoring of chemical interactions of biomolecules [4], diagnostic imaging [5], and therapeutics [6]. Some of the fluorescent dyes selectively localize and stain a cellular target organelle such as mitochondria, lysosomes, endoplasmic reticulum, or Golgi apparatus. Besides, some ligands possess dual behaviour when interacting with DNA, such as a fluorescence enhancement or quenching based on the flanking base sequence [7,8]. In specific, the most widely used dyes for nuclear staining are 4′,6-diamidino-2-phenylindole (DAPI) [9], ethidium bromide [10] and Hoechst 33258 [11], which emit strong fluorescence when bound to

DNA. Among the fluorescent probes [12,13], phenoxazine and its derivatives interact with DNA mainly *via* noncovalent interactions or by π-π stacking which render stability to these planar polycycles. [14,15]. Analytical techniques such as X-ray crystallography [16], mass spectrometry [17], UV-visible [18] and fluorescence spectroscopies [19] are employed to study the binding properties of fluorophores with DNA.

In this perspective, Nile Blue (NB) derivatives possess the required structural framework for intercalation with biomolecules, mainly due to low toxicity and good sensitivity for DNA quantification purposes [20]. Moreover, NB was used as a marker for the detection of DNA in gel electrophoresis experiments [21,22]. Continuing our research towards the synthesis and photophysical studies of fluorescent molecules [23-31], the present work is focused to study the DNA interaction with a set of benzo[*a*]phenoxazinium dyes bearing chlorinated terminals at the 2- and 5-positions of the heterocycle. Additionally, we evaluated the influence of methyl, hydroxyl or the amino group terminals at 5-position of the polycyclic systems [31] and photophysical studies of the interaction with DNA and in agarose gel electrophoresis assays were studied.

## 2. Experimental

### *2.1. Materials*

Tris(hydroxylmethyl)aminomethane (Tris) and HCl (37%) was purchased from Sigma-Aldrich. Natural double-stranded salmon sperm DNA was obtained from Invitrogen as a 10 mg/mL aqueous solution with an average size of 2000 bp. Tris/Acetic acid/EDTA (TAE) buffer solution was obtained from BioRad Laboratories GmbH. The strength of the 1× solution: 40 mM Tris, 20 mM acetic acid, 1 mM EDTA was used. Stock solutions of salmon sperm DNA was prepared in 10 mM Tris-HCl buffer (pH=7.4), with 1 mM EDTA. The purity of DNA was checked by the absorption spectrum and the ratio of absorbance $A_{260}/A_{280}$ = 1.95 (good-quality DNA has $A_{260}/A_{280}$ ratio higher than 1.8) [32]. The DNA concentration in number of bases (or phosphate groups, [P]) was determined from the molar absorption coefficient ε=6600 $M^{-1}cm^{-1}$ at 260 nm [33]. Appropriate amounts of $10^{-4}$ M ethanolic solutions of compounds **1**-**6** were added to DNA solutions at the desired concentrations. The solutions were stored for 24 h to stabilize. All other chemical reagents and solvents (spectroscopic grade) were commercially available and used without further purification.

*2.2. Synthesis of benzo[a]phenoxazinium chlorides **1**-**6***

Benzo[*a*]phenoxazinium chlorides **1**-**6** (Figure 1) was synthesised by condensation of the corresponding nitrosophenol hydrochloride, 5-(bis(3-chloropropyl)amino)-2-nitrosophenol hydrochloride (compounds **1** and **2**) or 5-((3-chloropropyl)amino)-2-nitrosophenol hydrochloride compounds **3** to **6**), with *N*-alkylated naphthalen-1-amine or *N*- and *O*-alkylated 5-aminonaphthalen-2-ol, namely *N*-propylnaphthalen-1-amine, 6-(3-chloropropoxy)-*N*-propyl naphthalen-1-amine, 3-(naphthalen-1-ylamino)propan-1-ol, $N^1$-(naphthalen-1-yl)propane-1,3-diamine hydrobromide in acidic (HCl) ethanol, as previously reported [31]. The required nitrosophenol was obtained by nitrosation of the corresponding 3-aminophenol precursor with sodium nitrite and hydrochloric acid in aqueous ethanol [34]. All the intermediates and benzo[*a*]phenoxazines obtained were characterised by $^{1}$HNMR, $^{13}$CNMR and HRMS [31].

<**Insert Figure 1**>

*2.3. Instrumentation and methods*

Absorption spectra (200-800 nm) were recorded on a Shimadzu UV-3101PC UV/vis/NIR spectrophotometer. Fluorescence measurements were performed using a Spex Fluorolog 2 spectrofluorometer, equipped with double monochromators in both excitation and emission, Glan-Thompson polarizers and temperature-controlled cuvette holder. Spectra were corrected for the instrumental response of the system.

Fluorescence quantum yields ($\Phi_F$) were determined using the standard method (Equation (1)) [35,36] with Oxazine 1 in ethanol as reference, $\Phi_r = 0.11$ [37]:

$$\Phi_s = \frac{A_r F_s n_s^2}{A_s F_r n_r^2} \Phi_r \quad (1)$$

where $A$ is the absorbance at the excitation wavelength, $F$ the integrated emission area and $n$ the refraction index of the solvents used. Subscripts (r) and (s) denotes the reference and sample compounds.

The steady-state fluorescence anisotropy, $r$, is calculated by Equation (2),

$$r = \frac{I_{VV} - G I_{VH}}{I_{VV} + 2G I_{VH}} \quad (2)$$

where $I_{VV}$ and $I_{VH}$ are the intensities of the emission spectra obtained with vertical and horizontal polarization, respectively (for vertically polarized excitation light), and G = $I_{HV}/I_{HH}$ is the instrument correction factor, where $I_{HV}$ and $I_{HH}$ are the emission intensities obtained with vertical and horizontal polarization (for horizontally polarized excitation light).

Fluorescence quenching studies with iodide ion were modelled using Equation (3),

$$\frac{I_0}{I} = \frac{f_{int}\varepsilon_{int}\Phi_{int} + (1-f_{int})\varepsilon_w\Phi_w^0}{f_{int}\varepsilon_{int}\Phi_{int} + (1-f_{int})\varepsilon_w\Phi_w} \quad (3)$$

where $I_0$ and $I$ are the fluorescence intensities in the absence and presence of quencher, respectively; $f_{int}$ is the fraction of intercalated molecules in DNA and $\Phi_{int}$ their fluorescence quantum yield; $\Phi_w^0$ and $\Phi_w$ represent the fluorescence quantum yields (in water) in the absence or presence of quencher, respectively; $\varepsilon_w$ and $\varepsilon_{int}$ are the molar absorption coefficients of the dye in water or when intercalated in DNA, respectively.

Using $\alpha = \frac{\varepsilon_w\Phi_w^0}{\varepsilon_{int}\Phi_{int}}$, equation (3) simplifies to Equation (4),

$$\frac{I_0}{I} = \frac{f_{int} + (1-f_{int})\alpha}{f_{int} + (1-f_{int})\alpha\Phi_w/\Phi_w^0} \quad (4)$$

and, by application of the Stern-Volmer relation, we obtain

$$\frac{I_0}{I} = \frac{f_{int} + (1-f_{int})\alpha}{f_{int} + (1-f_{int})\alpha/(1+K_{SV}[KI])} \quad , \quad (5)$$

$K_{SV}$ being the Stern-Volmer constant and [KI] the concentration of potassium iodide.

The sonication experiments were performed using an ultrasonicator QSonica Misonix S-4000. The electrophoresis apparatus was a BioRad Power Pac 300 running at an electric potential difference of 100 V. The distance between the electrodes in the electrophoretic chamber was 20 cm such that the applied electrical field was 5 V/cm. Solutions of benzo[*a*]phenoxazinium chlorides **1**-**6** with DNA at a molar ratio of [phosphate]/[dye]=5 (P/D) were prepared using 12 µL of salmon sperm DNA in Tris-HCl buffer solution, [P] = 0.0025 M, 6 µL of 1 mM solution of compounds **1**-**6** in ethanol, 10 µL of glycerin/water 1:1 as sample loading buffer and 32 µL of TAE buffer. A volume of 40 µL of the resulting solution was loaded in wells of the gel which was obtained from 0.3% solution of agarose gel in TAE buffer. The amount of DNA in each well was 6 µg. In regular time intervals, the

electrophoresis run was interrupted and images were captured with a digital camera. The graphics was done using the ImageJ software.

## 3. Results and discussion

### *3.1 Photophysical studies of benzo[a]phenoxazinium chlorides **1**-**6***

Our previous investigations on benzo[*a*]phenoxazinium chlorides showed that these compounds are involved in an acid-base equilibrium, the later being affected by proton acceptor solvents depending on the substituent, particularly at 5-amino position [23,25,27]. In ethanol, the absorption spectra are dominated by the acidic form ($AH^+$) and a ~ 100 nm blue shifted neutral form (A) [23]. The fluorescence spectra of the dyes show a broad band at 600 nm due to the basic form and another at 660 nm corresponding to the acidic form with higher quantum yields [23]. These fluorescence bands exhibited a bathochromic shift upon changing the solvent from ethanol to water which is a typical behaviour of π-π* electronic transition [23,24]. At 470 nm, the basic form is preferentially excited, while at 575 nm the opposite situation occurs. Photophysical studies of the compounds **1**-**6** were already published and follow these general characteristics [31]. In order to evaluate the photophysical behaviour of chlorinated benzo[*a*]phenoxazinium derivatives **1**-**6** (Figure 1) as non-covalent markers for DNA, absorption and emission spectra were measured at a constant fluorophore concentration ($2\times10^{-6}$ M) while systematically changing the concentration of DNA.

#### *3.1.1 UV–vis absorption and fluorescence studies in the presence of DNA*

Figure 2 shows the normalised absorption spectra as a function of P/D ([DNA Phosphate]/[Dye] molar ratio).

< **Insert Figure 2**>

The compounds can be categorized into two groups based upon their absorption spectra in the presence of DNA. Compounds **1**, **3**, **5** and **6** showed normal acidic form ($AH^+$) absorption, while the second set of compounds **2** and **4**, exhibited broader bands, indicative of aggregates and/or basic neutral form (A). Acid-base equilibria influenced the interaction of molecules with DNA as the affinity might be different for the acidic and basic forms [40,41]. As these compounds in water have a tendency to form H-aggregates [23,25], the $pK_a$ values

are ill-defined. Nevertheless "$pK_a$" values were determined in anhydrous ethanol media and are in the range 4-5 [42]. But the presence of trace amount of water promotes the formation of the acidic form so that the color of solutions in "normal" ethanol is blue instead of the reddish tone observed in anhydrous ethanol and the $pK_a$ values increase from 5 to 6.5 range [25]. Thus, in aqueous media the acid-base equilibria is normally completely shifted to the acid form. Accordingly, the studied compounds **1**, **3**, **5** and **6**, disregarding the presence of aggregates, only show the acid form in aqueous media.

For compounds **1**, **3** and **5**, the main variations of absorption spectra with P/D molar ratio are an initial red shift of the right edge of the spectra, followed by smaller spectral shifts for all of the dyes until P/D = 4. Nextly, at P/D = 5, remarkable spectral changes occur, which correspond to a reduction of full width at half maximum (FWHM) with an additional red shift, that is smaller for compound **3**. The initial variation for dyes **1**, **3** and **5** can be explained by electrostatic binding [43,44] through a higher local polarity felt by the compounds, thereby inducing a red shift, while the formation of H-aggregates results in an enlargement towards the blue region of the spectrum. This type of behaviour has been reported earlier [25,26]. H-aggregates are non-fluorescent, resulting in a decrease of fluorescence quantum yield, as observed in Figure 3.

The behaviour of absorption spectra above P/D = 5 indicates a probable intercalation process, which is confirmed by a corresponding red shift in fluorescence emission and a stabilization of the fluorescence quantum yield (Figure 3), as shown and proved for similar compounds in previous studies [26].

< **Insert Figure 3**>

The fluorescence emission of compound **3** shows an additional band near 600 nm, which only occurs in the presence of DNA. This band corresponds to the neutral basic form [23,25]. This distinct behavior may correspond to a different location of this fraction of compound **3** molecules in DNA, probably at the grooves. It is noteworthy that compound **1**, possessing two chlorinated terminal side chains, does not show the basic form emission, indicating that groove binding is hindered by di-substitution at 9-position of the heterocycle. The fact that compound **5** also does not exhibit the basic form emission is an indication that a polar substituent in 5-position also disfavors groove binding.

Compound **6**, possessing high DNA affinity, above P/D=2 show the same type of absorption spectrum with no evidence of aggregation, but red-shifted from the one in Tris-

HCl buffer. This absence of aggregation is responsible for the lack of initial decrease in fluorescence quantum yield with P/D in opposition to what was observed for compounds **1**, **3** and **5** (Figure 3).

The observed rise in fluorescence quantum yield with increasing P/D can be explained by the corresponding decrease of the blue edge in emission spectrum, because emission in the 600 nm region corresponds to the neutral form, which is ten times lower quantum yield than the cationic form ($AH^+$) [23]. The red-shifted emission observed at high P/D values also indicates that compound **6** intercalates between the DNA base pairs. As a result, this compound tends to interact with DNA mainly by groove and intercalative binding. Moreover, among this set of benzo[*a*]phenoxazinium chlorides (**1**, **3**, **5** and **6**), the necessary P/D value for intercalation is between 3 and 10.

The other set of benzo[*a*]phenoxazinium chlorides (**2** and **4**) has an additional chlorinated side chain at 2-position of the polycyclic system. The absorption spectra (Figure 2) exhibit oscillating behavior between aggregates and the acid cationic form, with the appearance of the basic neutral form in the absence of DNA. The fluorescence quantum yields are very low, especially for compound **4**. No significant spectral variations are observed for compound **2** which has two chlorinated side chains at position 9, whereas for compound **4** a reduction of the blue half of the spectrum is observed with no significant red shift (Figure 3). From these observations it seems that compounds with side chains at 2-position interact very little with DNA and mainly through groove binding. For compound **2,** the decrease of quantum yield occurs above P/D=10 (Figure 3) but no significance can be attributed as the emission spectral shape remains the same and the corresponding variations in the absorption spectra (Figure 2) would point to an increase of quantum yield: decrease in the fraction of absorption at 575 nm that is a consequence of higher fraction of the acid form as can be confirmed in the spectra and inset for this compound in figure 2.

In order to better follow the appearance of the basic form emission in the presence of DNA, fluorescence spectra at 470 nm excitation were measured for compounds **1**, **3**, **5** and **6**, for which the signal-to-noise ratio is still reasonable. The results are presented in Figure 4.

< **Insert Figure 4**>

It can be observed that the basic form only appears for compounds **3** and **6**, as already identified in fluorescence spectra obtained at 575 nm excitation. However, the behaviour of these two compounds is distinct. In compound **3**, it is the acidic form that is mainly excited,

while the spectrum for compound **6** gets completely dominated by the basic form, even though its presence in absorption spectrum (Figure 2) is not prominent. Additional bands were seen in the spectral region 510 – 570 nm, which relative intensity changes with DNA content. These bands were previously observed for some of these compounds in AOT w/o microemulsions and, through *ab initio* calculation, were attributed to a tautomeric form stabilized by the chloride counter ion [31]. In DNA, the counter ion is probably a nearby phosphate group of the polynucleotide chain. It is interesting to note that, for compounds **1**, **3** and **5**, the relative emission intensity at 510 nm increases with DNA content, reaching a plateau at *ca.* P/D = 5, while for compound **6** it reaches a maximum at P/D = 2. Ignoring the presence of the Raman peak, the relation between the bands at 510 nm and 550 nm is different for compound **6** than for the other studied compounds. Taking into account all the results presented so far, it can be concluded that the tautomerization of the acid cationic form is more favorable upon intercalation. The distinct behavior of compound **6** must be a consequence of the terminal amine functional group, which is expected to be in $NH_3^+$**.**$Br^-$ form, and this additional localized charge should enhance the interaction with DNA through direct electrostatic attraction to negative phosphate groups. This interaction is predictable to be more important in groove binding of the basic neutral form, as it would function as an electrostatic anchor with the backbone of the molecule lying down within the DNA kinks.

*3.1.2 Effect of temperature in the interaction with DNA*

Compound **5**, with a hydroxyl group as terminal of the substituent at 5-amino position, is the one that exhibits the highest fluorescence intensity and absorption in presence of DNA. Thus, further confirmation of intercalation of compound **5** in DNA was obtained by the study of DNA denaturation with temperature (Figure 5A). At high temperature, double stranded DNA separates in two complementary single strand chains (*ss*-DNA). The process is partially reversible, as the *ss*-DNA chain dynamics hinders the exact recombination of the nucleotide base pairs [26,38]. At P/D=100, compound **5** shows a blue shift in the absorbance spectrum upon heating at 70 ºC, which can be interpreted as compound molecules being detached from the DNA helix to the solution. Next, upon cooling, only a partial recovery is observed, which is consistent with a lower number of available intercalation sites that result from incomplete DNA renaturation.

< **Insert Figure 5**>

*3.1.3 Fluorescence quenching studies with iodide ion*

Further evidence can be obtained from fluorescence quenching assays using iodide ion as quencher (Figure 5B), as the fraction of compound molecules that intercalates in DNA is protected from close contact with the negatively charged quencher molecules. The quenching process is expected to be trough heavy atom effect on the intersystem crossing non-radiative process [39]. A negative curvature results in the usual Stern-Volmer plot, corresponding to a less efficient quenching [39]. This effect was modelled by equations (3) to (5) (see Experimental part). The theoretical curve shown in Figure 5B corresponds to 79% intercalated molecules and a quenching constant of 3.95 $M^{-1}$, with $\alpha$=10.8. This result confirms that intercalation is the preferred form of interaction with the nucleic acid at P/D=100.

*3.1.4 Fluorescence anisotropy measurements*

In order to gain further insight on the interaction of benzo[*a*]phenoxazinium chlorides **1**-**6** with DNA and confirm that intercalation occurs, fluorescence (steady-state) anisotropy measurements at 575 nm excitation were performed (Figure 6). Fluorescence anisotropy, *r*, deviates from its intrinsic value, $r_0$, as a result of possible molecular rotation before emission occurs. In fact, the anisotropy value increases with the rotational correlation time of the fluorescent molecule and, therefore, with the viscosity of the fluorophore environment through the Perrin equation [39].

< **Insert Figure 6**>

For compounds **1** and **5** at low P/D, the fluorescence anisotropy has the same profile as in the absence of DNA (Figure 6). This indicates that either the compounds are not intercalated between DNA base pairs, or the binding mode detected by fluorescence does not significantly prevent molecular rotation. As these compounds exhibited changes in absorption and fluorescence spectra at low DNA content (Figures 2 and 3), it can be concluded that part of the molecules interact with DNA and are loosely bound, such that the intrinsic anisotropy, $r_0$, created by excitation with polarized light, is lost by molecular rotation. The fraction of molecules that form H-aggregates is not detected by this technique. Thus, the initial red shift observed in fluorescence spectra at low P/D values (Figure 3) corresponds to the emission of

compound molecules electrostatically-bound to DNA, that remain un-aggregated and easily rotatable. The decrease of fluorescence quantum yield can be mainly due to the static process of aggregate formation, since a decrease in excited state lifetime would result, through the Perrin equation [39], in an increase in fluorescence anisotropy which is not observed.

Compounds **2** and **6** mainly exhibit an increase in fluorescence anisotropy at low P/D values. This is a confirmation that groove binding occurs with these compounds, as molecular rotation is restricted when molecules are inserted inside DNA kinks. A much larger restriction occurs upon DNA intercalation. The large values of anisotropy (the maximum $r_0$ value is 0.4) observed at high P/D ratios confirm, with the exception of compound **2**, the intercalation of the studied compounds into DNA double strands.

It can be observed that compound **2** does not show significant changes in fluorescence anisotropy upon increasing the DNA amount. The increasing anisotropy with emission wavelength is probably due to the formation of non-ordered aggregates with a large aggregation number. The lack of interaction with DNA was previously seen in absorption and fluorescence data (Figures 2 and 3). For compound **4**, which is similar to compound **2** but with only one chlorinated side chain, a significant increase in anisotropy was observed at high P/D, indicating an intercalation behavior that was not evident from fluorescence and absorption spectra.

*3.2 Gel electrophoresis assays*

In order to assess the potential of benzo[*a*]phenoxazinium chlorides **1**-**6** as DNA markers and their binding strength, agarose gel electrophoresis assays were performed, keeping in mind the application of these compounds as alternatives to the commonly used ethidium bromide marker (a very mutagenic compound). Figure 7 shows the results obtained for compound **5** at P/D ratio of 5 and 1. It is observed that only for the higher P/D the migrating DNA remains stained.

< **Insert Figure 7**>

The positive charge of the studied compounds makes them to travel in the opposite direction to DNA. The electrostatic binding of the dye to DNA is not strong enough to compensate the opposing travelling directions. On the contrary, intercalation binding allows the cationic dyes to remain associated with DNA during the electrophoretic migration. Upon

successive re-equilibration with “clean” buffer, the amount that stays associated with DNA decreases, resulting in fading of the DNA band.

< **Insert Figure 8**>

< **Insert Figure 9**>

As in a previous study [30], the curves shown in Figures 8 and 9 were obtained by transforming the image, taken with a digital camera at fixed time intervals, into a gray scale and averaging the pixel intensity (0-dark; 255-white) in each lane, as a function of the distance from the wells where the DNA solutions were initially placed. At P/D = 5, the migration of DNA to the positive pole was seen as blue travelling bands for all compounds that faded after 30 min of electrophoresis run. If compounds were not bound to DNA, the migration would have occurred in the opposite direction towards the negative pole. Therefore, strong binding of these compounds to DNA was confirmed.

With DNA, compound **5** migrated more slowly than all the other compounds, which showed similar migrating velocities. As the bands were migrating, a tail was left behind on the gel (Figure 7). This tailing can be an indication that some dye molecules separate from DNA and start migrating in the opposite direction, spreading within the gel [30]. Compounds **1**, **2**, **3** and **5** show a less extent of tailing, observed in the curves of Figure 8 by a lower intensity before the peak corresponding to the DNA band. The dye Nile Blue, which belongs to the same family of compounds, has proven to be useful in DNA electrophoretic separations [22]. However, in this work, the tested experimental setup involves only the labeling of DNA rather than staining the whole gel and the applied electric field is three times lower.

Furthermore, to test the feasibility of the studied compounds **1**-**6** as markers in DNA size separations, an electrophoresis assay was performed with the same DNA, but downsized using ultrasonication at 80 W for one hour. It can be seen that the migration velocities are higher for a downsized DNA chain (as expected) and a leading shoulder appears that reflects a disperse population of even smaller DNA fragments (Figure 9). This shoulder is more prominent for compound **6**. The electrophoresis experiments also reveal that compound **2** which, from spectroscopic results, seemed to have a weak interaction with DNA, also binds strongly to the nucleic acid especially for the sonicated sample.

## 4. Conclusions

In summary, benzo[*a*]phenoxazinium chlorides **1**-**6** possessing chlorinated side chains at 9- and 2-positions with different terminal groups at 5-position (methyl, hydroxyl and amino) were evaluated for their ability to interact with DNA. Photophysical studies revealed that all compounds interact strongly with DNA, intercalation occurring at P/D exceeding 3, with an exception for compound **2**. The hydroxyl terminal of benzo[*a*]phenoxazinium dye **5** enhances the interaction with DNA, whereas substitution at 2-position for compounds **2** and **4** has the reverse effect. Compound **6** with $NH_2$.HBr terminal showed a peculiar behavior, with a high affinity towards DNA and a significant amount of groove binding. Furthermore, in agarose gel electrophoresis experiments with ultrasonicated and non-sonicated DNA, compounds **1**-**6** exhibited efficient binding to DNA, avoiding the need of staining the whole gel.


## Acknowledgements

Thanks are due to Fundação para a Ciência e a Tecnologia (FCT, Portugal) and FEDER (European Fund for Regional Development)/COMPETE-QREN-EU for financial support to Research Centres CQ/UM [PEst-C/QUI/UI0686/2013 (FCOMP-01-0124-FEDER-037302)] and CFUM [PEst-C/FIS/UI0607/2013 (F-COMP-01-0124-FEDER-022711)]. The Post-doctoral grant to B. R. Raju (SFRH/BPD/62881/2009) is also acknowledged to FCT, POPH-QREN, FSE.


## References


[1] T. Terai, T. Nagano, Pflugers Arch - Eur J Physiol 465 (2013) 347-59.

[2] S. Dey, L.A. Ambattu, P.R. Haria, M.R. Rekha, K. Sreenivasan, Polymer 75 (2015) 25-33.

[3] D. Vasudevan, A. Trinchi, S. G. Hardin, I.S. Cole, J. Lumin., 166 (2015) 88-92.

[4] S. Deshayes, G. Divita, Prog. Mol. Biol. Transl. Sci. 113 (2013) 109-143.

[5] H-B. Wang, H-D. Zhang, Y. Chen, Y-M. Liu, Biosens. Bioelectron. 74 (2015) 581-586.

[6] L. Bu, B. Shen, Z. Cheng, Adv. Drug. Deliv. Rev. 76 (2014) 21-38.

[7] A. Rajendran, V. Thiagarajan, B. Rajendar, S. Nishizawa, N. Teramae, Biochim. Biophys. Acta 1790 (2009) 95-100.

[8] A. Rajendran, C. Zhao, B. Rajendar, V. Thiagarajan, Y. Sato, S. Nishizawa, N. Teramae Biochim. Biophys. Acta 1800 (2010) 599-610.
[9] J. Kapuscinski, Biotech Histochem. 70 (1995) 220-33.
[10] J. Yguerabide, A. Ceballos, Anal. Biochem. 228 (1995) 208-220.
[11] B.C. Hyman, T.W. James, Anal. Biochem. 131 (1983) 205-210.
[12] K.E. Erkkila, D.T. Odom, J.K. Barton, Chem. Rev. 99 (1999) 2777-2796.
[13] A.K. Williams, S.C. Dasilva, A. Bhatta, B. Rawal, M. Liu, E.A. Korobkova, Anal. Biochem. 422 (2012) 66-73.
[14] D. Chadar, S.S. Rao, A. Khan, S.P. Gejji, K.S. Bhat, T. Weyherm¨ullerb, S.Salunke-Gawali RSC Adv., 5 (2015) 57917-57929.
[15] A. Bolognese, G. Correale, M. Manfra, A. Lavecchia, E. Novellino, S. Pepe, J. Med. Chem. 49 (2006) 5110-5118.
[16] N.H. Hopcroft, A.L. Brogden, M. Searcey, C.J. Cardin, Nucleic Acids Res. 34 (2006) 6663-6672.
[17] J.S. Brodbelt, Annu. Rev. Anal. Chem. 3 (2010) 67-87.
[18] S.T. Saito, G. Silva, C. Pungartnik, M. Brendel, J. Photochem. Photobiol. B 111 (2012) 59-63.
[19] W. Chen, N.J. Turro, D.A. Tomalia, Langmuir 16 (2000) 15-19.
[20] Q.-Y. Chen, D.-H. Li, H.-H. Yang, Q.-Z. Zhu, J.-G. Xu, Y. Zhao, Analyst 124 (1999) 901-906.
[21] Y.I. Yang, H.Y. Hong, I.S. Lee, D.G. Bai, G.S. Yoo, J.K. Choi, Anal. Biochem. 280 (2000) 322-324.
[22] S. Adkins, M. Burmesiter, Anal. Biochem. 240 (1996) 17-22.
[23] V.H.J. Frade, M.S.T. Gonçalves, P.J.G. Coutinho, J.C.V.P. Moura, J. Photochem. Photobiol. A 185 (2007) 220-230.
[24] C.M.A. Alves, S. Naik, P.J.G. Coutinho, M.S.T. Gonçalves, Tetrahedron Lett. 50 (2009) 4470-4474.
[25] C.M.A. Alves, S. Naik, P.J.G. Coutinho, M.S.T. Gonçalves, Tetrahedron 65 (2009) 10441-10452.
[26] C.M.A. Alves, S. Naik, P.J.G. Coutinho, M.S.T. Gonçalves, Tetrahedron Lett. 52 (2011) 112-116.
[27] S. Naik, C.M.A. Alves, P.J.G. Coutinho, M.S.T. Gonçalves, Eur. J. Org. Chem. (2011) 2491-2497.
[28] A.D.G. Firmino, M.S.T. Gonçalves, Tetrahedron Lett. 53 (2012) 4946-4950.

[29] A.D.G. Firmino, B.R. Raju, M.S.T. Gonçalves, Eur. J. Org. Chem. (2013) 1506-1514.
[30] B.R. Raju, S. Naik, P.J.G. Coutinho, M.S.T. Gonçalves, Dyes Pigm. 99 (2013) 220.
[31] B.R. Raju, A.D.G. Firmino, A.L.S. Costa, P.J.G. Coutinho, M.S.T. Gonçalves, Tetrahedron 69 (2013) 2451-2461.
[32] Y. Cao, X.W. He, Spectrochim. Acta A: Mol. Biomol. Spectrosc. 54 (1998) 883-892.
[33] E. Renault, M.P. Fontaine-Aupart, F. Tfibel, M. Gardes-Albert, M. Gardes-Albert, E. Bisagni, J. Photochem. Photobiol. B: Biol. 40 (1997) 218-227.
[34] M.L. Crossley, P.F. Dreisbach, C.M. Hofmann, R.P. Parker, J. Am. Chem. Soc. 74 (1952) 573-578.
[35] G.A. Crosby, J.N. Demas, J. Phys. Chem. 75 (1971) 991-1024.
[36] S. Fery-Forgues, D. Lavabre, J. Chem. Educ. 76 (1999) 1260-1264.
[37] R. Sens, K.H. Drexhage, J. Lumin. 24 (1981) 709-712.
[38] F. Michel, J. Mol. Biol. 89 (1974) 305-326.
[39] B. Valeur, "Molecular Fluorescence – Principles and Applications", Wiley-VCH, Weinheim (2002).
[40] S. Mukherjee, P. Das, S. Das J. Phys. Org. Chem. 25 (2012) 385-393.
[41] T. Deb, P.K. Gopal, D. Ganguly, P. Das, M. Paul, M.B. Saha, S. Paul, S. Das RSC Adv., 4 (2014) 18419-18430.
[42] B.R. Raju, M.M.T. Carvalho, M.I.P.S. Leitão, P.J.G. Coutinho, M.S.T. Gonçalves, Dyes and Pigments 132 (2016) 204, 212.
[43] S. Maiti, K. Sasmal, S.S. Sinha, M. Singh Ecotox. Environ. Safe 124 (2016) 248-254.
[44] S. Maiti, K. Sasmal, S.S. Sinha, M. Singh Cosmetics 2 (2015) 313-321.

## Figure Captions

**Figure 1.** Structures of benzo[*a*]phenoxazinium chlorides **1**-**6**.

**Figure 2**. Normalised absorption spectra of compounds **1**-**6** in buffered (Tris-HCl, pH = 7.4) aqueous solutions of DNA. Each panel is identified with the compound number. The curves are identified by the corresponding P/D values. The insets show maximum absorption (circles) and absorption at 575 nm (squares) as a function of P/D. The gray curve corresponds to the absence of DNA. For P/D=0.5, 1, 2, 3, 4, 5, 10, 50, 100 the color of the curves are respectively red, blue, green, magenta, cyan, yellow, purple, olive and orange. The same color code was used for figures 3 and 4.

**Figure 3**. Normalised fluorescence intensity at 575 nm excitation of compounds **1**-**6** in buffered (Tris-HCl, pH = 7.4) aqueous solutions of DNA. Each panel is identified with the compound number. The curves are identified by the corresponding P/D value. The insets show the fluorescence quantum yield as a function of P/D. The gray curve corresponds to the absence of DNA.

**Figure 4**. Normalised fluorescence intensity at 470 nm excitation of compounds **1**, **3**, **5** and **6** in buffered (Tris-HCl, pH = 7.4) aqueous solutions of DNA. Each panel is identified with the compound number. The curves are identified by the corresponding P/D value. The insets show the normalised fluorescence intensity at 510 nm as a function of P/D. The gray curve corresponds to the absence of DNA.

**Figure 5**. (A) Temperature effect on the absorption spectra of compound **5** in DNA solution with P/D = 100. (B) Fluorescence quenching by iodide of compound **5** in DNA solution with P/D = 100.

**Figure 6**. Fluorescence anisotropy spectra at 575 nm excitation of compounds **1**-**6** in buffered (Tris-HCl, pH = 7.4) aqueous solutions of DNA, for P/D = 0, 0.5 and 100. Each panel is identified with the compound number.

**Figure 7**. Agarose gel electrophoresis assay of salmon sperm DNA marked with compound **5** without DNA (top lane), with P/D = 5 (middle lane) and P/D = 1 (bottom lane).

**Figure 8**. Agarose gel electrophoresis assays of salmon sperm DNA marked with compounds **1**-**6**. In each picture, two white lines mark the position of the wells, the order of the compounds in the lanes are, from top to bottom, in same order as in the legend of the graph. Top image after 5 min run; bottom image after 10 min run. The graph plots the pixel intensity in gray scale (0-black; 255-white) for each line as a function of distance from the well.

**Figure 9**. Agarose gel electrophoresis assays of ultrasonicated salmon sperm DNA marked with compounds **2**, **4**, **5** and **6**. In each picture, two white lines mark the position of the wells, the order of the compounds in the lanes are, from top to bottom, in same order as in the legend of the graph. Top image after 5 min run; middle image after 10 min run; bottom image after 20 min run. The graph plots the pixel intensity in gray scale (0-black; 255-white) for each line as a function of distance from the well.

**Figure 1**.

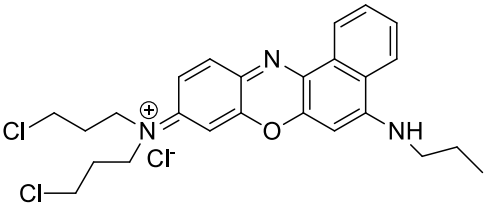


**1**

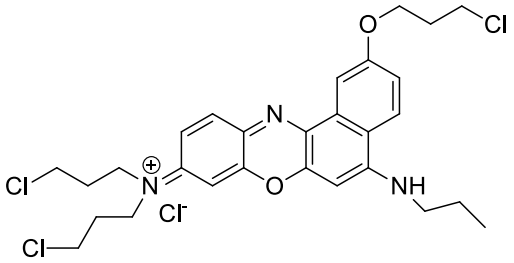


**2**

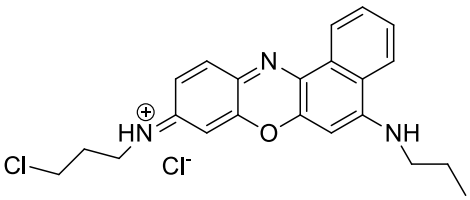


**3**

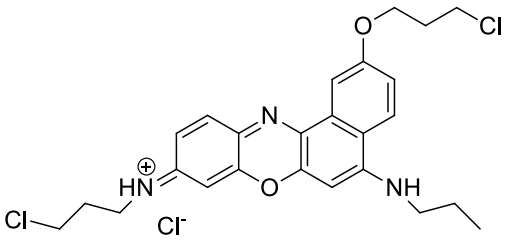


**4**

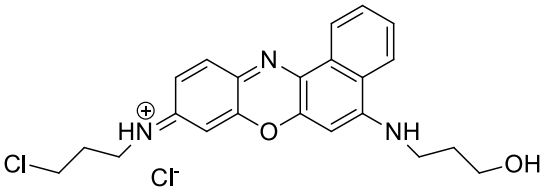


**5**

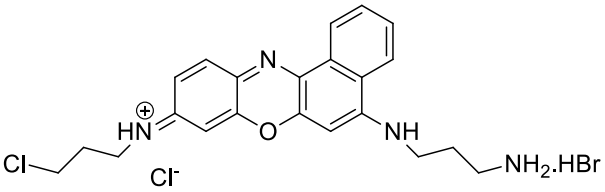


**6**

**Figure 2.**

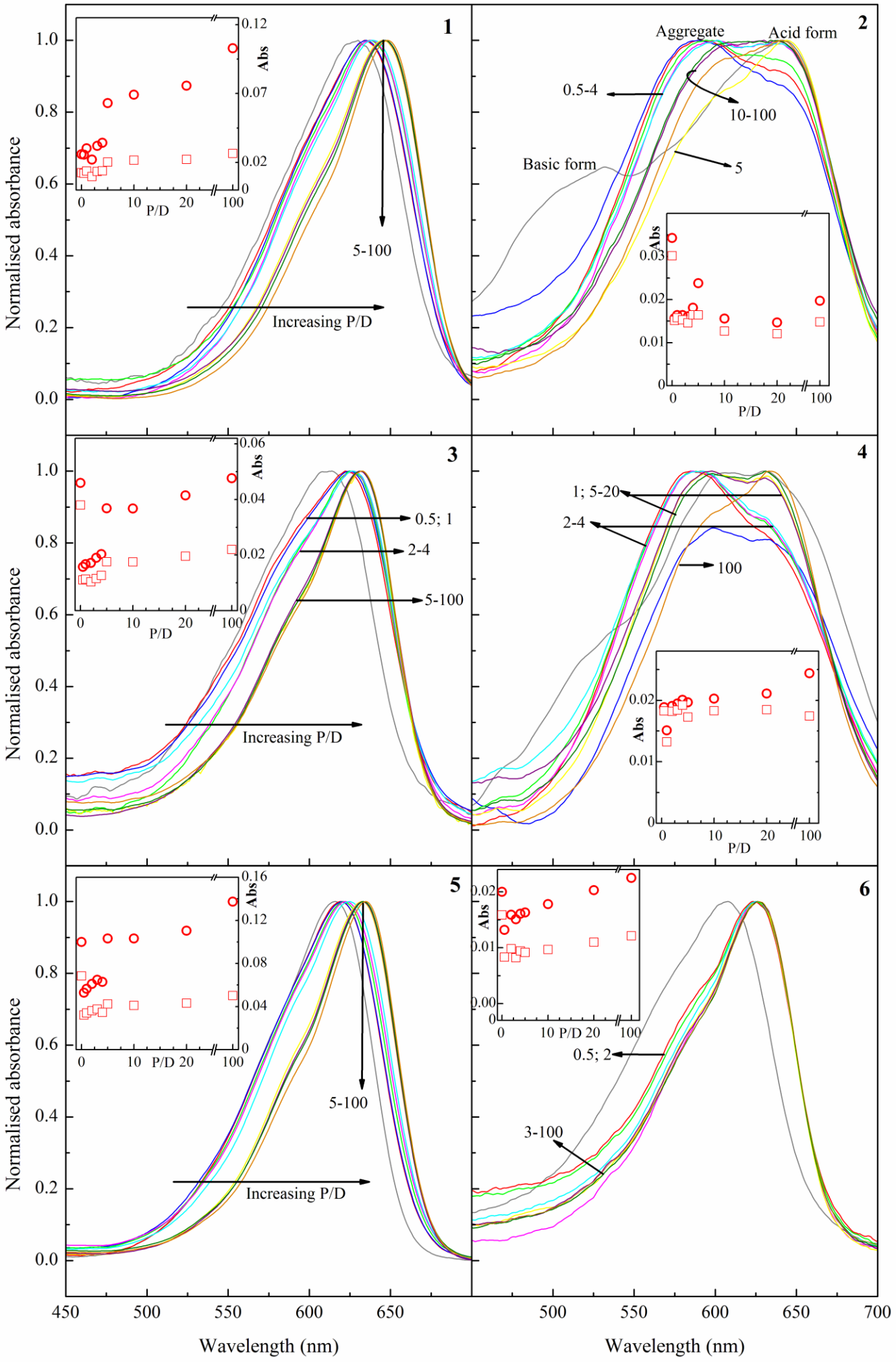
1
5-100
Increasing P/D
Abs
P/D
2
Aggregate
Acid form
0.5-4
10-100
Basic form
5
3
0.5; 1
2-4
5-100
Increasing P/D
4
1; 5-20
2-4
100
5
5-100
Increasing P/D
6
0.5; 2
3-100
Normalised absorbance
Wavelength (nm)

**Figure 3.**

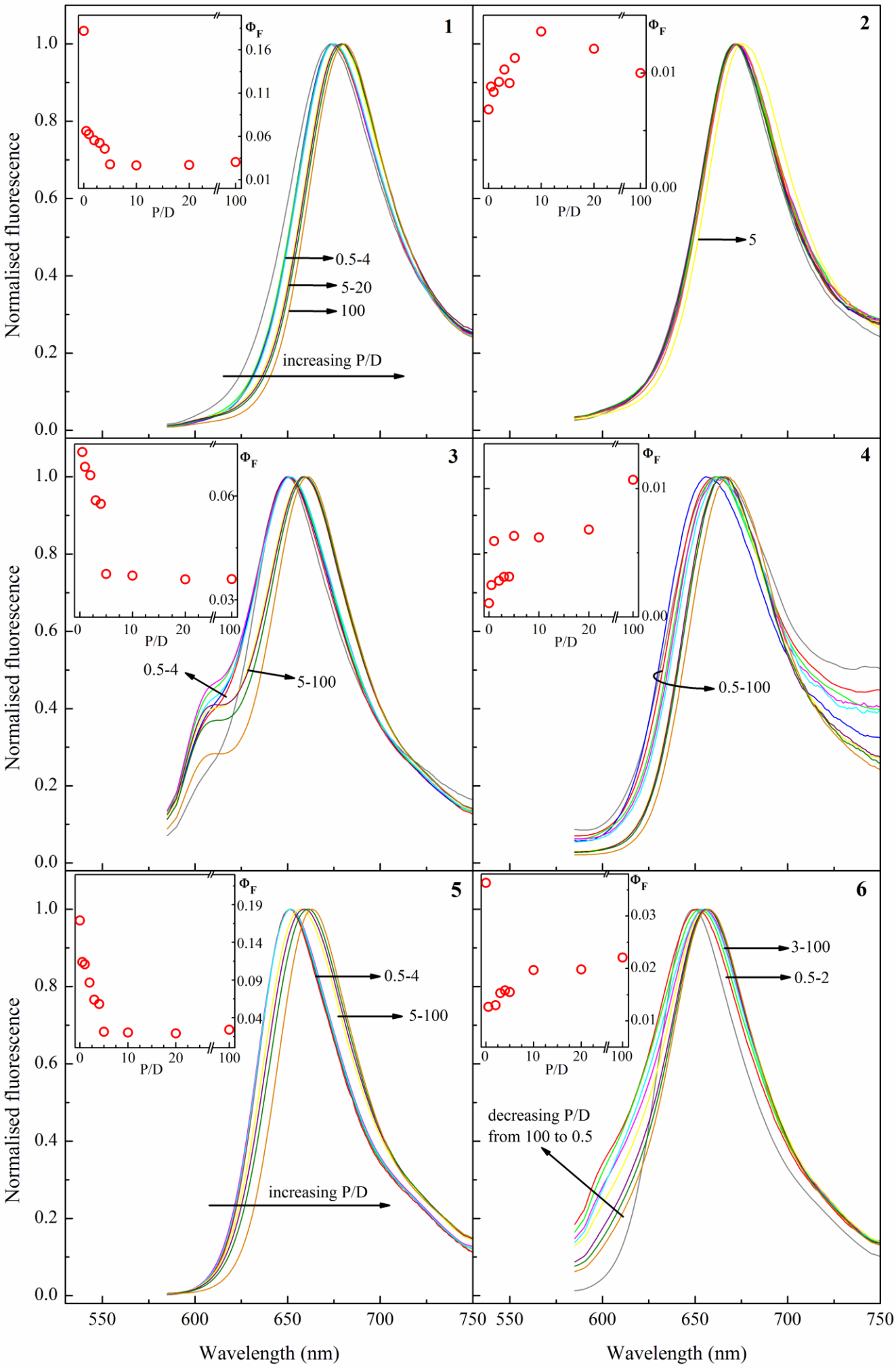
1
2
3
4
5
6
Normalised fluorescence
Wavelength (nm)
P/D
ΦF
0.5-4
5-20
100
increasing P/D
5
0.5-100
5-100
3-100
0.5-2
decreasing P/D
from 100 to 0.5

**Figure 4**.

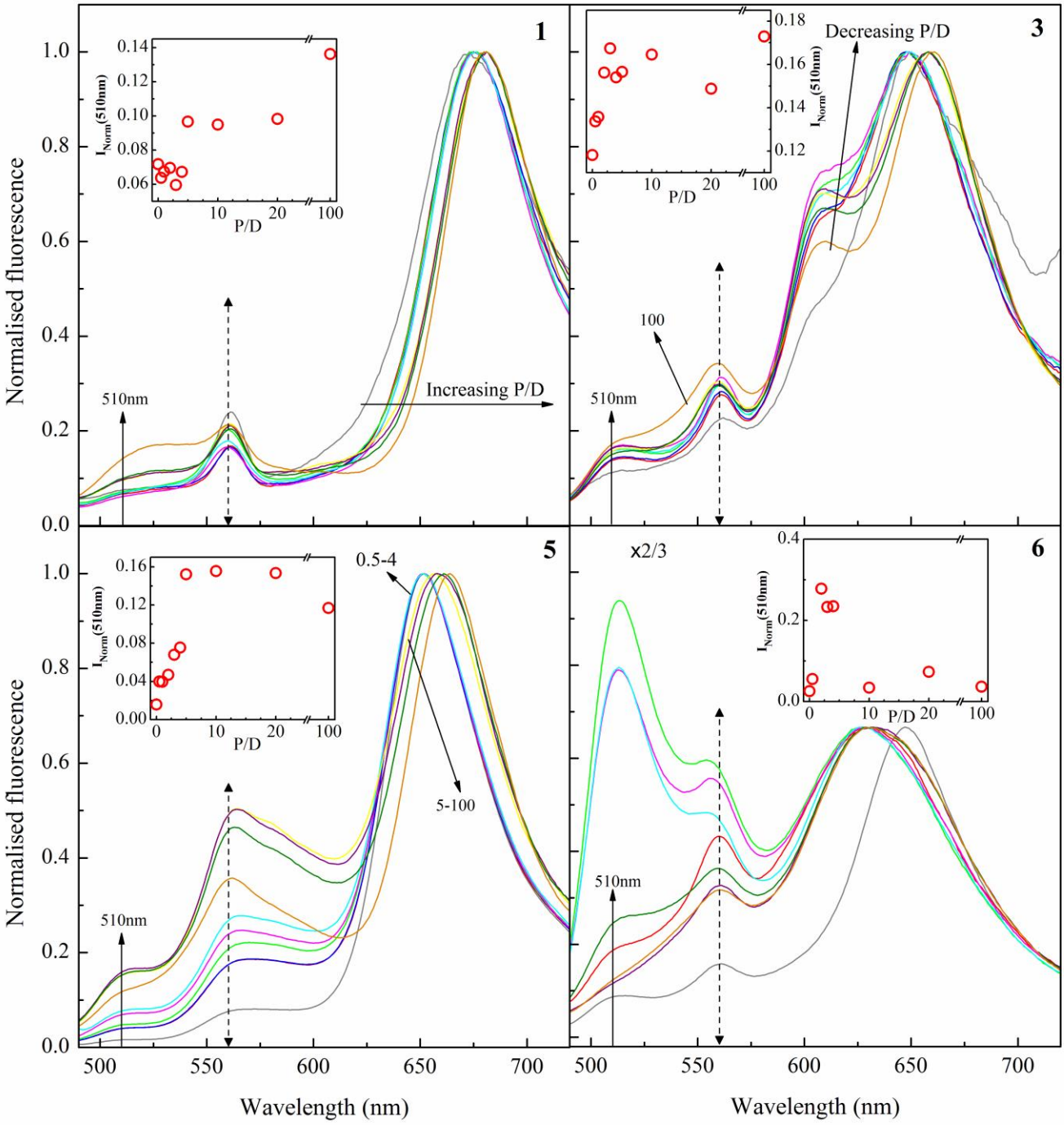
1
3
5
6
Normalised fluorescence
Wavelength (nm)
510nm
Increasing P/D
Decreasing P/D
100
0.5-4
5-100
x2/3
P/D
I_Norm(510nm)

**Figure 5**.

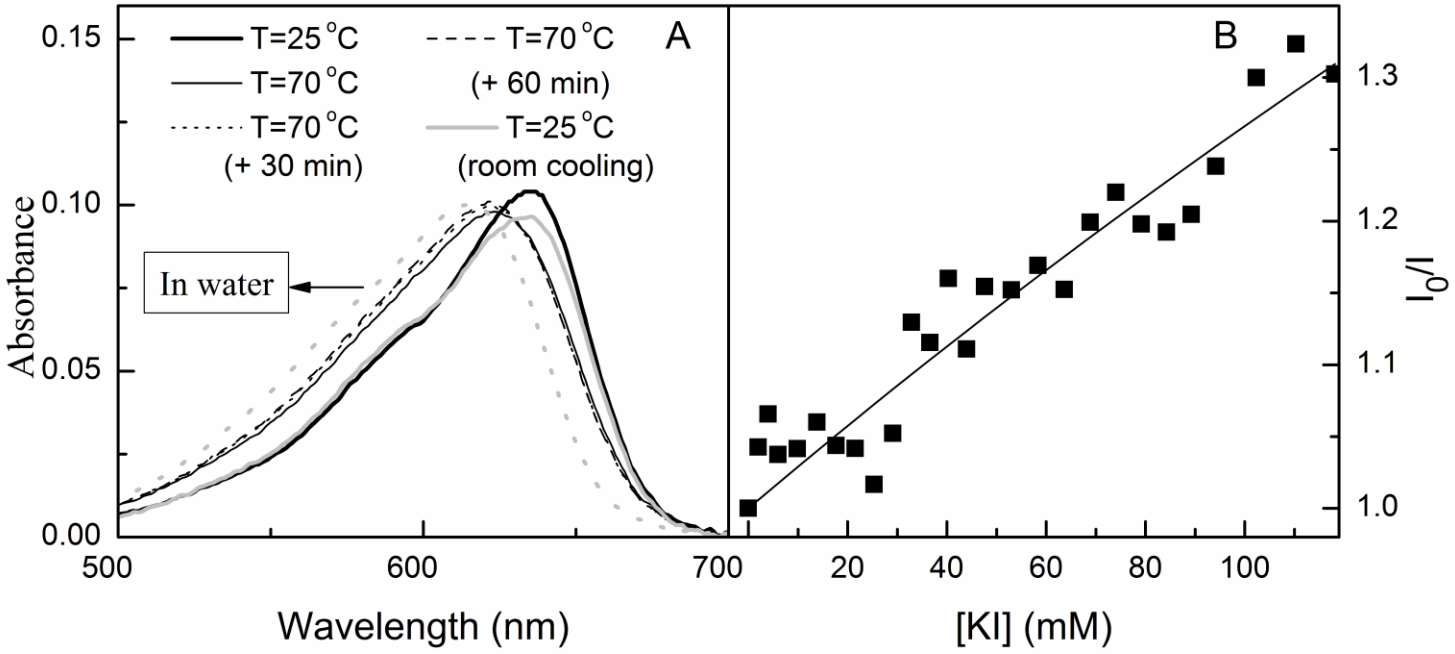


**Figure 6**.

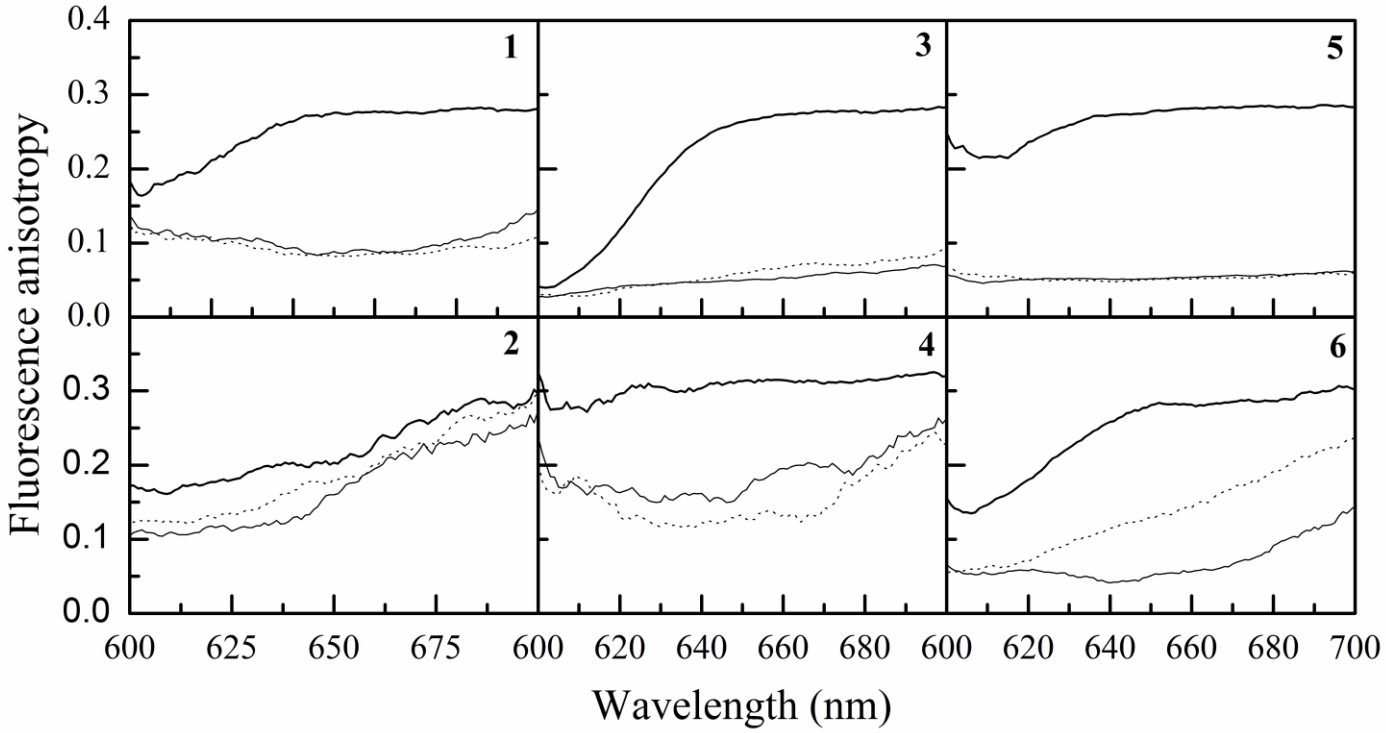

**Figure 7**.

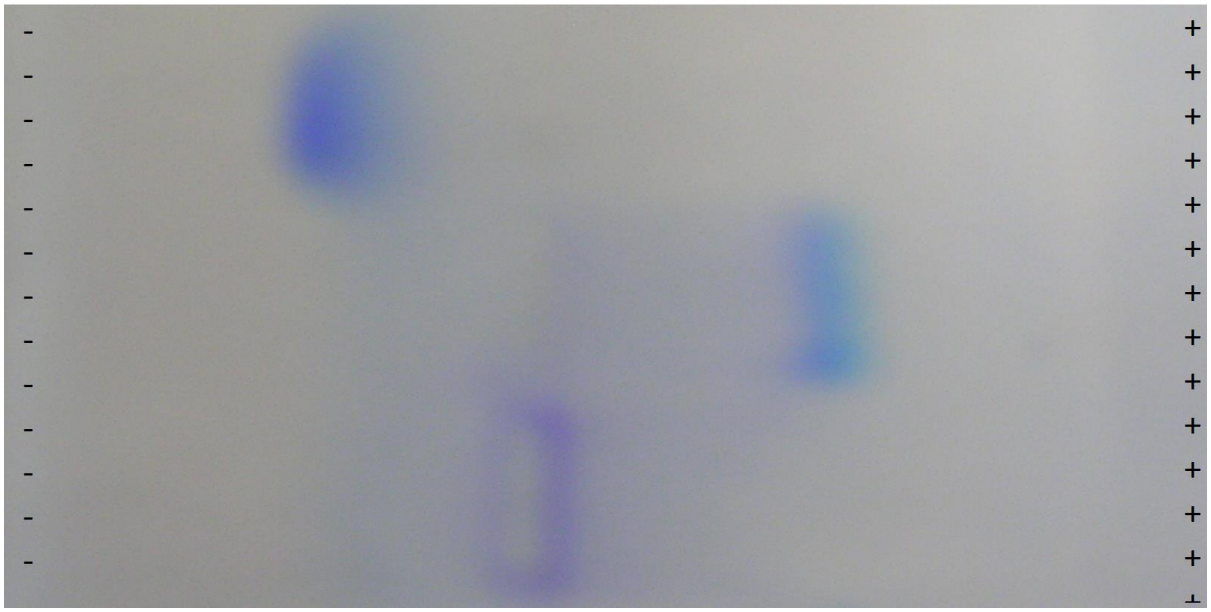

**Figure 8**.

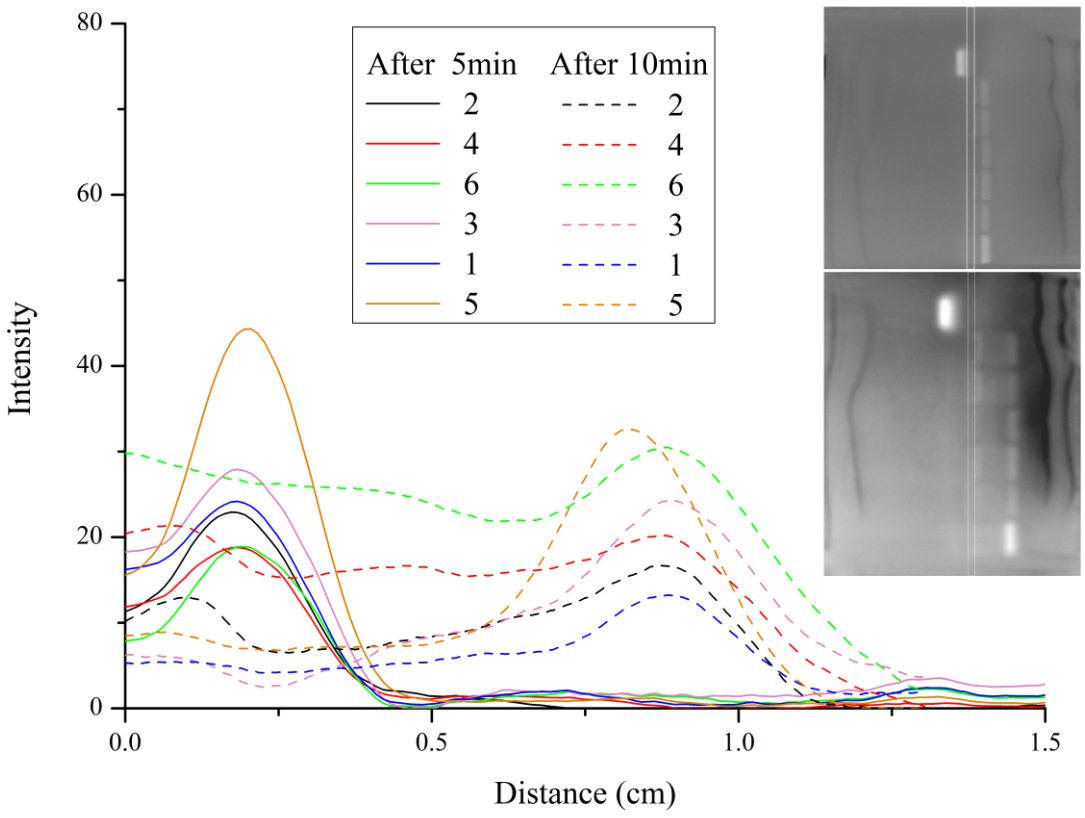

**Figure 9**.

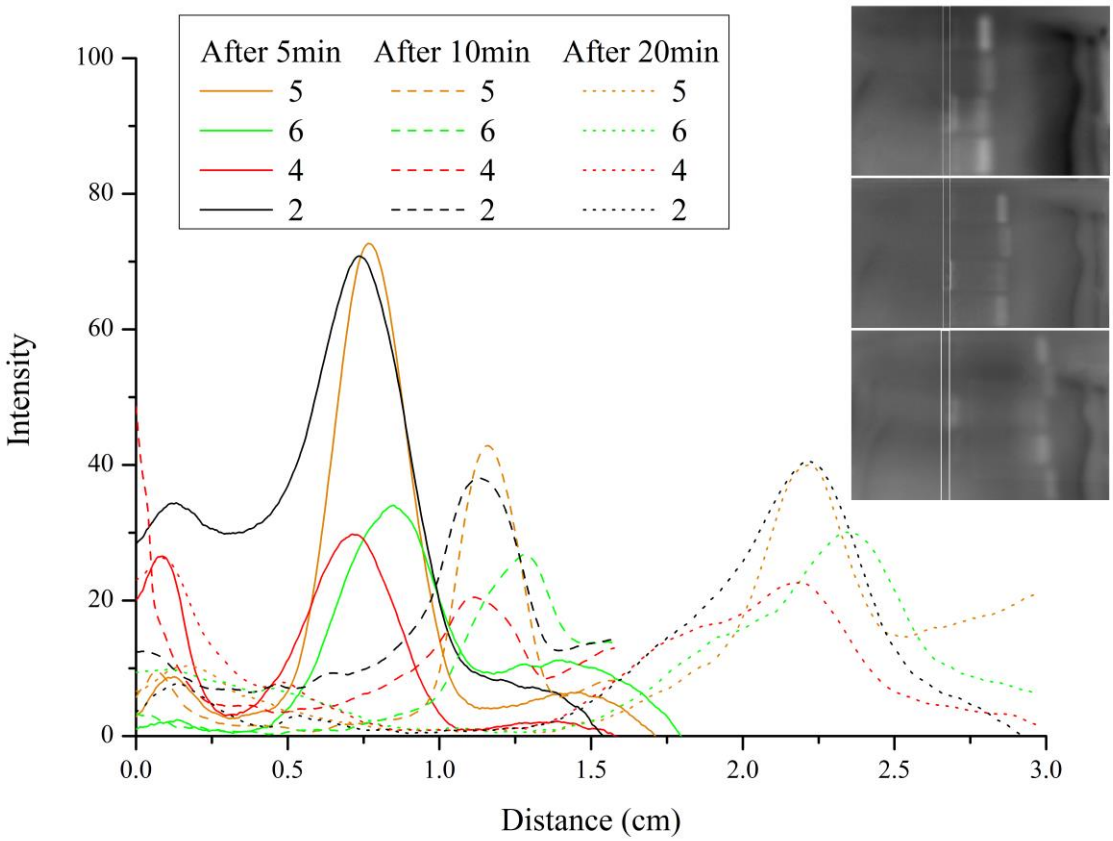
After 5min
After 10min
After 20min
5
6
4
2
Intensity
Distance (cm)
0
20
40
60
80
100
0.0
0.5
1.0
1.5
2.0
2.5
3.0